Clays and Clay Minerals, Vol. 66, No. 2, 104–113, 2018.

CRYSTAL GROWTH OF LAYERED SILICATE GRAFTED WITH ORGANIC GROUPS ON MONODISPERSE SPHERICAL SILICA PARTICLES

MASAHIRO YAMAUCHI AND TOMOHIKO OKADA*

Department of Chemistry and Materials Engineering, Shinshu University, Nagano 380-8553, Japan

Abstract—Control of the structure and morphology of clay crystals presents a challenge in the synthesis of materials for adsorption and catalysis. In the present study, direct crystallization of a phyllosilicate grafted with organosilyl (methylsilyl and phenylsilyl) groups on the surface of monodisperse spherical silica particles (2.6 μm) is reported. Methyl- and phenyltriethoxysilanes were allowed to react hydrothermally in a Teflon-lined autoclave with silica, $MgCl_2$, and LiF in the presence of urea for 2 or 4 days. X-ray diffraction patterns revealed that the fine platy particles formed were a trioctahedral hectorite-like layered silicate. Greater temperature (150ºC) was required to achieve homogeneous coverage of the original spherical silica particles with the hectorite-like particles. The diameter of the initial silica grains increased slightly to 3.0 μm after the hydrothermal reactions, while the original spherical shape and size distribution were maintained. Solid-state ^{29}Si nuclear magnetic resonance analyses confirmed that the presence of resonances attributed to the *R*Si(OMg)$(OSi)_2$ and *R*Si(OMg)(OH)(OSi) (*R* = methyl or phenyl) environments of the silicon proved the formation of covalent bonds between phyllosilicate sheets and the organic moieties. The crystallinity of the layered silicates increased when the reactions ran for a longer time (4 days).

Key Words—Grafting, Hectorite, Heterogeneous Nucleation, Hydrothermal Synthesis, Organosilane.

INTRODUCTION

Clay-like synthetic layered solids have been investigated from the viewpoints of selective adsorption, molecular separation, and controlled release using their two-dimensional interlayer spaces (Ogawa and Kuroda, 1995; Cool and Vansant, 2004; Rogez *et al*., 2011; Okada *et al*., 2012a, 2014; Chhowalla *et al*., 2013; Okada and Ogawa, 2017). The morphology of a material (*e.g.* the particle-size distribution and shape) is also important with a view to enhancing the applicability of the material. Hybridization with solid supports can be used in flow systems to solve a problem whereby fine powder often causes a decrease in contact efficiency owing to a drop in pressure. Fine crystals of layered solids have been mounted on the surface of supports *via* heterogeneous nucleation reactions (Okada, 2018); solid supports have often been used as sources of the layered solids, whereas the other reactants were supplied by the solution medium. Combinations of solid substrates and reactants present in solution can lead to the formation of various types of fine crystal such as titanosilicate-silica fibers (Pérez-Carvajal *et al*., 2013), (Ni, Zn)/Al layered double hydroxide (LDH)-Al_2O_3 plates (Chen *et al*., 2006; Yamaguchi *et al*., 2006; Zhang *et al*., 2008; Katagiri *et al*., 2009), and (Mg, Zn)/Al LDH−Al_2O_3 fibers (Zhang *et al*., 2013, 2014). Owing to the partial dissolution of the support, the growth of crystals preserves the shape of the support, which is referred to as a 'sacrificial template' or 'self-template.'

Synthetic smectites, which possess swelling properties similar to those of natural smectites, have been obtained *via* hydrothermal methods for various applications because of their cation-exchange ability, lack of colored impurities, fine powder form, and structural/compositional versatility. Cation-exchange reactions modify the interlayer space to create various useful microenvironments with features such as hydrophobicity (Carrado *et al*., 2001), pillared structures with robust microporosity (Pinnavaia *et al*., 1984; Kloprogge, 1998), and soft microstructures with specific chemical affinities (Okada *et al*., 2015a, 2017). Organosilyl groups, on the other hand, are used to modify silicate layers *via* covalent bonding by sol-gel processes (post-grafting) and hydrothermal reactions with organosilane reagents (one-pot formation). The post-grafting onto surface silanol groups of layered silicic acids has been reported *via* silylation reactions (Ruiz-Hitzky and Rojo, 1980; Ruiz-Hitzky *et al*., 1985; Thiesen *et al*., 2000, 2002; Ogawa *et al*., 1998). The one-pot formation of a phyllosilicate-like structure (direct incorporation of organic functionalities) can also be achieved by using organosilanes as silicon sources under both non-hydrothermal (Jaber *et al*., 2002) and solvothermal conditions (Fukushima and Tani, 1995, 1996; Burkett *et al*., 1997; Whilton *et al*., 1998; da Fonseca *et al*., 1999, 2000a,

* E-mail address of corresponding author:
tomohiko@shinshu-u.ac.jp
DOI: 10.1346/CCMN.2018.064097

This paper was originally presented during the session 'NT-11. Material's Challenges for Clay Scientist' during ICC 2017

2000b; Carrado *et al*., 2001; Fujii *et al*., 2003; Jaber *et al*., 2005).

Direct crystallization of fine crystals of hectorite-like (Okada *et al*., 2012b, 2015b, 2016a, 2016b, 2016c) and saponite-like (Okada *et al*., 2015c) layered silicates have been reported using amorphous silica as a solid support and which acted as a sacrificial template and functioned as the source of the layered silicates by the partial dissolution of silica. The size and shape of the silica substrate (*e.g.* fibers, spheres, hollow structures) affect directly the characteristics of the final product, and unique and useful functions have been reported, including facile recovery from aqueous media (Okada *et al*., 2012b, 2016b), topochemical intercalation (Okada *et al*., 2015b), filtration (Okada *et al*., 2016a), rapid chiral discrimination (Okada *et al*., 2016c), and controlled release (Okada *et al*., 2015c). Amorphous silica hence offers many advantages as a heterogeneous nucleation medium for the development of hierarchically designed supports. The morphological control of covalently linked phyllosilicates using the sacrificial template method has, however, not been studied. Heterogeneous nucleation reactions of an organic–inorganic lamellar composite on monodisperse spherical colloidal silica particles (2.6 μm) are reported here. The aim of the study was to prepare composites, on spherical silica, which contain interlayer exchangeable cations and organic functionalities (methyl and phenyl groups) in a hectorite-like structure.

EXPERIMENTAL

Materials

Magnesium chloride hexahydrate (98.0%), lithium fluoride (99.9%), urea (99.0%), methylene blue (MB) (95.0%), calcium chloride (95%), and sodium chloride (99.5%) were purchased from Wako Pure Chemical Industries, Ltd., Osaka, Japan. Monodisperse spherical silica particles with a grain size of 2.6 μm (KE-P250, Nippon Shokubai Co., Ltd., Osaka, Japan), methyltriethoxysilane (MTEOS; Shin-Etsu Chemical Co., Ltd., Tokyo, Japan), and phenyltriethoxysilane (PTEOS; Shin-Etsu Chemical Co., Ltd.) were used as sources of layered silicates. All these chemicals were used as received.

Crystal growth of layered silicate grafted with organic groups on monodisperse spherical silica

A typical molar ratio of LiF:$MgCl_2$:SiO_2:urea in the starting mixture was 0.13:0.19:1.0:1.0. Urea (1.0 g), $MgCl_2 \cdot 6H_2O$ (0.66 g), and LiF (0.058 g) were dissolved in 30 mL of water (Merck Millipore water: resistivity >15 Mω). The resulting solution was mixed with an aqueous suspension of spherical silica particles (1.0 g in 20 mL of water) which contained a certain amount of MTEOS or PTEOS (0.04, 0.3, or 0.5 mol/L mol SiO_2) using a mechanical homogenizer at 4600 rpm for 30 min at room temperature. The molar ratio of the organosilane to SiO_2 in the starting mixture was varied, as summarized in Table 1. The slurry was transferred to a Teflon-lined autoclave and heated to 100 or 150ºC for 2 or 4 days. The products were named as Me/Ph-*n*-*t*-L/H, as listed in Table 1, where *n* and *t* refer to the molar ratio of the organosilane and the reaction period in days, respectively. In the sample names, Me and Ph indicate that the added organosilane was MTEOS or PTEOS, respectively. The reaction temperatures indicated in the list by L and H correspond to 100 and 150ºC, respectively. The autoclave was spun at 15 rpm in a hydrothermal synthesis reactor (Hiro Company, Yokohama, Japan) during the heat treatment. The slurry was then cooled in an ice bath and centrifuged at $1400 \times g$ for 10 min, and the precipitate was then collected and dried at 50ºC.

Polymerization of each organosilane was conducted to compare the structures of the layered silicates by mixing MTEOS or PTEOS (5 mmol) in an aqueous solution of NaOH (0.1 mol/L) for 24 h under magnetic stirring at 60ºC. The precipitate was collected by centrifugation at $1400 \times g$ for 10 min and then washed with water and dried at 50ºC.

Adsorption of MB from aqueous solution

The products (0.10 g) were allowed to react with 25 mL of aqueous MB solution (0.14–0.75 mM) in a glass vessel with reciprocal stirring for 1 day at 25ºC. To estimate the adsorption of MB to the vessel, blank samples containing 25 mL of aqueous MB solution with no adsorbents were also prepared. After centrifugation ($1400 \times g$, 15 min), the concentration of MB remaining in the supernatant was determined by UV visible spectroscopy (UV-2450PC spectrophotometer, Shimadzu, Kyoto, Japan) to determine the amount of MB adsorbed at the wavelength of 665 nm.

Table 1. Sample names and reaction conditions used for direct crystallization of organo-phyllosilicates on spherical silica particles.

Sample	Organo silane	Amount of organosilane (*vs.* 1 mol SiO_2)	Conditions
	MTEOS		
Me-0-4-H		0	150ºC, 4 days
Me-0.04-4-H		0.04	150ºC, 4 days
Me-0.04-2-H		0.04	150ºC, 2 days
Me-0.04-4-L		0.04	100ºC, 4 days
Me-0.04-2-L		0.04	100ºC, 2 days
Me-0.3-4-H		0.3	150ºC, 4 days
Me-0.5-4-H		0.5	150ºC, 4 days
	PTEOS		
Ph-0.04-4-H		0.04	150ºC, 4 days
Ph-0.3-4-H		0.3	150ºC, 4 days

https://doi.org/10.1346/CCMN.2018.064097 Published online by Cambridge University Press

Equipment

Scanning electron microscopy (SEM) images were captured using an Hitachi (Tokyo, Japan) SU-8000 field emission scanning electron microscope (operated at 10 kV) after osmium plasma coating of the samples. Powder X-ray diffraction (XRD) patterns were obtained using a Rigaku (Tokyo, Japan) RINT 2200 V/PC diffractometer with monochromatic CuKα radiation, operated at 20 mA and 40 kV in the range 2−70º2θ, where the sampling step and counting time were 0.01º2θ and 1.0 s, respectively. Solid-state ^{29}Si magic angle scanning (MAS) nuclear magnetic resonance (NMR) spectra were measured using a Bruker (Billerica, Massachusetts, USA) ASCEND 500 spectrometer equipped with a MAS probe (MASVTN 500SB BL4) at a resonance frequency of 99.36 MHz with a 90º pulse (high-power decoupling) and a recycle delay of 40 s. The spinning rate was 8 kHz. Thermogravimetric differential thermal analysis (TG-DTA) curves were recorded using a Rigaku TG8120 instrument in a temperature range from room temperature to 1000ºC at a heating rate of 10ºC/min using α-alumina as the standard material.

RESULTS AND DISCUSSION

Reaction time and temperature

The XRD patterns of the hydrothermal products are shown in Figure 1. In all cases, the reflections of the (110), (130), and (060) planes, which could be ascribed to hectorite, were observed (Okada *et al*., 2012b). At the reaction temperature of 100ºC, the (00*l*) reflection was absent owing to the poor crystallinity of the hectorite-like silicates, as shown in Figure 1a,c. The crystal developed along the direction of the *c* axis (Figure 1b,d,e) when the reaction temperature was changed to 150ºC, irrespective of the presence or absence of MTEOS in the starting mixture. By-products such as $Mg(OH)_2$ (41 and 53º2θ) shown in Figure 1a,b disappeared when the reaction period was extended from 2 to 4 days. The basal spacing of the MTEOS-free sample was 1.25 nm (Me-0-4-H: Figure 1e), which implies that a monomolecular hydration layer occupied the interlayer space. A slight increase in the basal spacing to 1.36 nm was observed on the addition of MTEOS (Figure 1c,d). The interlayer spacing was 0.40 nm, which was determined by subtracting the thickness of the silicate sheet (0.96 nm) (Bailey, 1988) from the basal spacing observed, and that value coincided with the size of methyl groups (0.4 nm) based on the molecular size of methane (Webster *et al*., 1998). Hydrolyzed MTEOS was, therefore, thought to be intercalated between the silicate layers.

The SEM images of the products are shown in Figure 2. Whole grains in the MTEOS-free product (Figure 2a) were essentially spherical with a size of ~3 μm. Platy fine particles were observed along the surface of the spheres, which indicated that a hectorite-like silicate grew on the silica spheres while maintaining their original shape. Such platy particles covered every grain of silica, and very few individual fine plates were found in the product. When MTEOS was added to the starting mixture, platy fine particles also appeared (Figure 2b−e). Because individual platy particles were not observed, direct crystallization of layered silicates on silica can be assumed to have occurred. At a higher

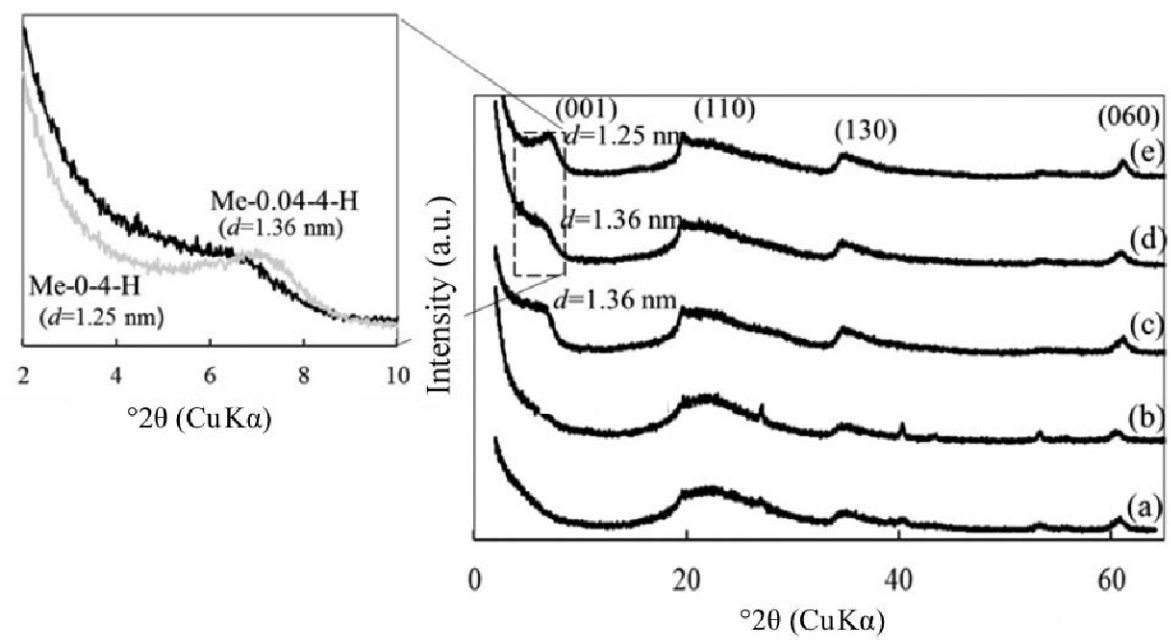

Figure 1. XRD patterns of: (a) Me-0.04-2-L, (b) Me-0.04-2-H, (c) Me-0.04-4-L, (d) Me-0.04-4-H, and (e) Me-0-4-H.

https://doi.org/10.1346/CCMN.2018.064097 Published online by Cambridge University Press

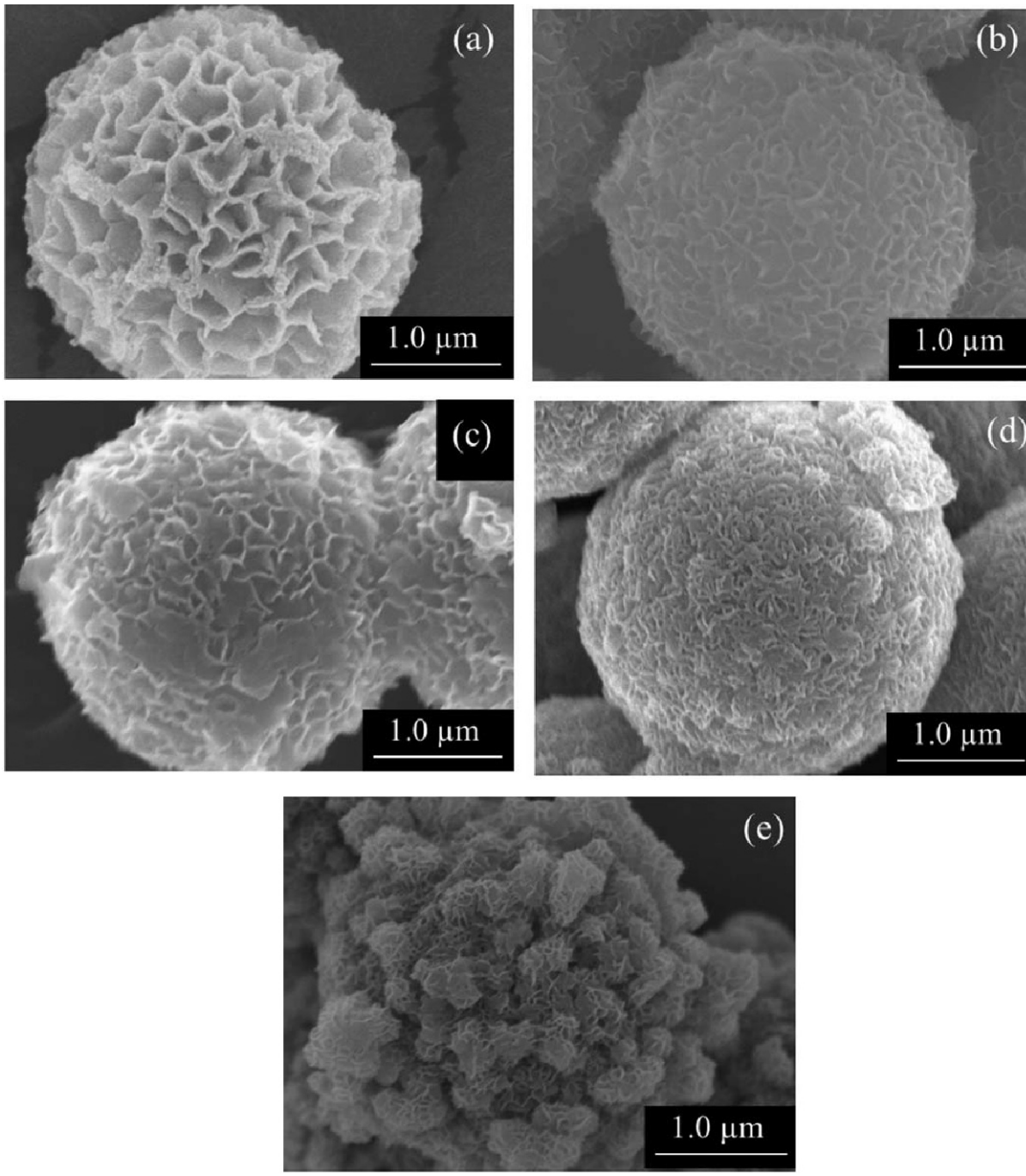

Figure 2. SEM images of: (a) Me-0-4-H, (b) Me-0.04-4-H, (c) Me-0.04-2-H, (d) Me-0.04-4-L, and (e) Me-0.04-2-L.

temperature (150ºC), the sizes of the resulting spherical grains (Figure 2b,c) were in the range 2.8–3.0 μm, whereas after treatment at 100ºC for 48 h (Figure 2e) a large number of smaller spheres (~0.2 μm) agglomerated on the original silica.

The dissolution of silica spheres has been reported to occur as an initial process before heterogeneous nucleation reactions of hectorite-like silicates (Okada *et al*., 2012b). The aging temperature is correlated directly with the solubility of the silica sol. Excess silica sol, which does not contribute to the formation of hectorite, has also been reported to lead to polymerization and the formation of silica spheres with smaller sizes (~0.2 μm) (Okada *et al*., 2016a). In the present system, the polymerization of silica probably occurred before the heterogeneous nucleation of layered fine particles at 100ºC. Excess silica sol was consumed by extending the reaction period to 96 h (Figure 2d), so that such smaller

https://doi.org/10.1346/CCMN.2018.064097 Published online by Cambridge University Press

silica particles disappeared to give a uniform grain-size distribution. The extension in the reaction period also resulted in the formation of relatively large platy crystals (Figure 2d). This enhancement of crystallization is thought to be related to condensation of the nuclei. The formation of nuclei has been postulated to take place at an initial stage of the reaction process, including the condensation of silica monomers onto previously formed octahedral sheets (Jaber and Miehe-Brendle, 2008). Some of these initial nuclei redissolved and recondensed to form true nuclei of layered silicates. The relative concentration of true nuclei is assumed to increase upon extension of the reaction period, as a result of continual condensation during aging over 4 days.

The increase in temperature to 150ºC also, presumably, affected the consumption of the excess silica sol, which led to an increase in oversaturation of the layered silicate crystals. A greater degree of oversaturation will facilitate crystal growth. As shown in Figure 2b, the aspect ratio (length of the plate) of the fine crystals was larger than that of those prepared at 100ºC (Figure 2d). The increase in degree of crystallinity was consistent with the XRD results (Figure 1).

Solid-state ^{29}Si MAS NMR analyses were performed to confirm that methyl groups had been grafted onto the silicate sheets. All the spectra (Figure 3) of the hydrothermal products contain Q*n* signals which were assigned to hectorite, *e.g.* $Q_3(Si(OMg)(OSi)_3)$ and $Q_2(Si(OMg)(OSi)_2(OH))$ at −94 and −86 ppm, respectively, in addition to $Q_4(Si(OSi)_4)$ at −110 ppm, which was assigned to the siloxane network (Carrado *et al*., 2000, 2002; Fujii and Hayashi, 2005). When MTEOS was present in the initial mixture (Figure 3a–d), T-type signals were also observed where silicon has three oxygen bridging atoms and one covalent bond with an organic moiety (R) (Sugahara *et al*., 1994). The positions of the T-type signals varied depending on the reaction temperature. At the lower temperature (100ºC; Figure 3a,c), signals that were assigned to $T_3(RSi(OSi)_3)$, $T_2(RSi(OH)(OSi)_2)$, and $T_1(RSi(OH)_2(OSi))$ were observed at −65, −58, and −50 ppm, respectively. These signals were located at the same positions as those for polymerized MTEOS (Figure 3e), which suggests that a proportion of MTEOS was not incorporated covalently into the silicate sheets at 100ºC. The T_2 and T_1 signals, on the other hand, shifted to −67 and −60 ppm, respectively, upon an increase in the reaction temperature to 150ºC (Figure 3b,d). These signals can be assigned to $T_2'(RSi(OMg)(OSi)_2)$ and $T_1'(RSi(OMg)(OH)(OSi))$ environments, respectively (Burkett *et al*., 1997; Whilton *et al*., 1998), which implies that methylsilyl groups were grafted onto phyllosilicate sheets. Extending the reaction period from 48 h (Figure 3b) to 96 h (Figure 3d) led to an increase in the intensity of the T_2' (grafting onto the interlayer siloxane layer) environment compared to the T_1' (grafting onto the crystal edge) environment, which is in accordance with an increase in crystallinity (Figure 1). The reaction temperature and reaction period were, therefore, optimized at 150ºC and 96 h, respectively, for the grafting of methylsilyl groups onto phyllosilicate sheets.

Amount of organosilane

The amount of MTEOS added to the starting mixture was increased from 0.04 to 0.3 mol/L mol SiO_2, and the reaction was conducted at 150ºC for 4 days. The XRD

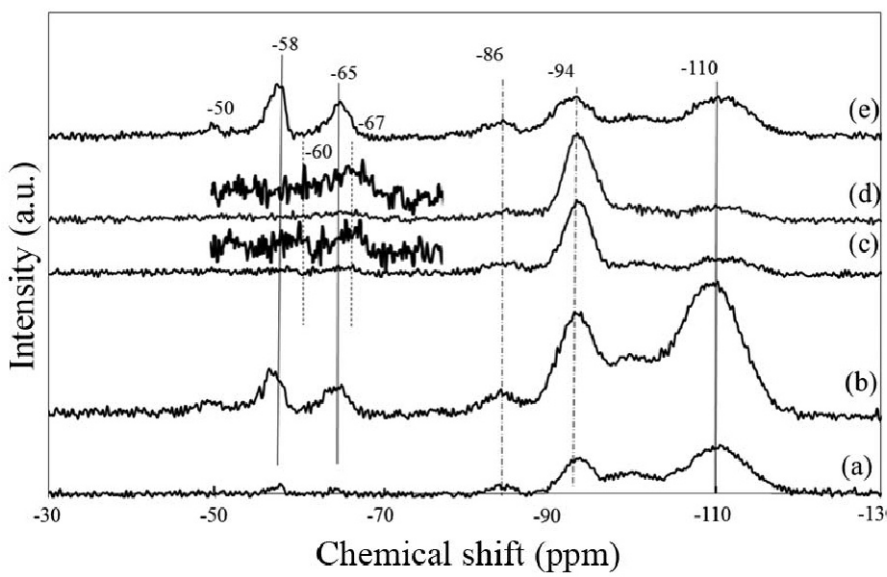

Figure 3. Solid-state ^{29}Si MAS NMR spectra of: (a) Me-0.04-2-L, (b) Me-0.04-2-H, (c) Me-0.04-4-L, (d) Me-0.04-4-H, and (e) a mixture of polymerized MTEOS and Me-0-4-H.

https://doi.org/10.1346/CCMN.2018.064097 Published online by Cambridge University Press

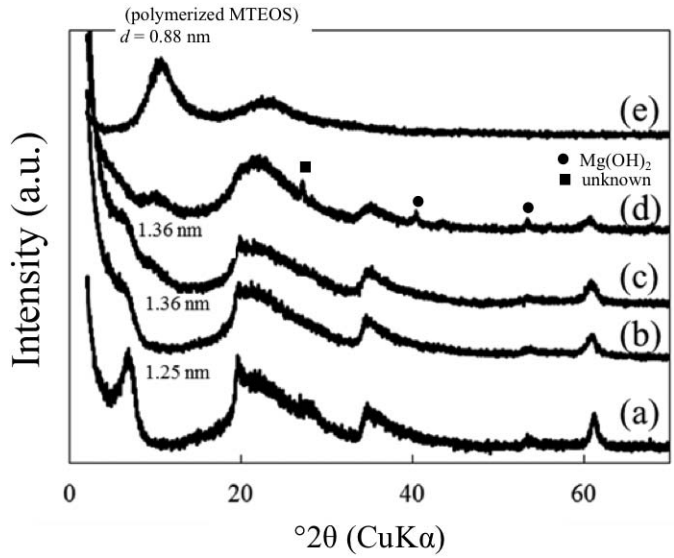

Figure 4. XRD patterns of: (a) Me-0-4-H, (b) Me-0.04-4-H, (c) Me-0.3-4-H, (d) Me-0.5-4-H, and (e) polymerized MTEOS.

pattern of the product (Me-0.3-4-H) is shown in Figure 4c together with that of the MTEOS-free product (Figure 4a). Diffraction peaks that could be ascribed to the (001), (110), (130), and (060) planes in hectorite were also observed for Me-0.3-4-H at 6.5º, 19.4º, 35.0º, and 61.0º2θ (CuKα), respectively, which suggests that a hectorite-like phyllosilicate formed in the presence of the increased amount of MTEOS. The basal spacing was 1.36 nm, which was the same as when the smaller amount of MTEOS was added (Me-0.04-4-H) and indicated the intercalation of methylsilyl groups with dense packing. A further increase in the amount of MTEOS to 0.5 mol/L mol SiO_2 resulted, however, in the precipitation of $Mg(OH)_2$ and polymerized MTEOS (Figure 4d). The XRD pattern of polymerized MTEOS (Figure 4e) included a diffraction peak at 10º2θ (CuKα), which was due to the lamellar structure of polymerized MTEOS.

The XRD patterns of the products obtained by the reactions with 0.04 and 0.3 mol/L PTEOS (Ph-0.04-4-H and Ph-0.3-4-H) are shown in Figure 5a,b. Reflections appeared that could be ascribed to the (001), (110), (130), and (060) planes of a hectorite-like layered structure, irrespective of the amount of PTEOS that was added. When compared with the pattern of polymerized PTEOS (Figure 5c), the position of each basal-plane reflection (6.8º2θ) was different because of the lamellar structure of the PTEOS polymer (7.3º2θ)

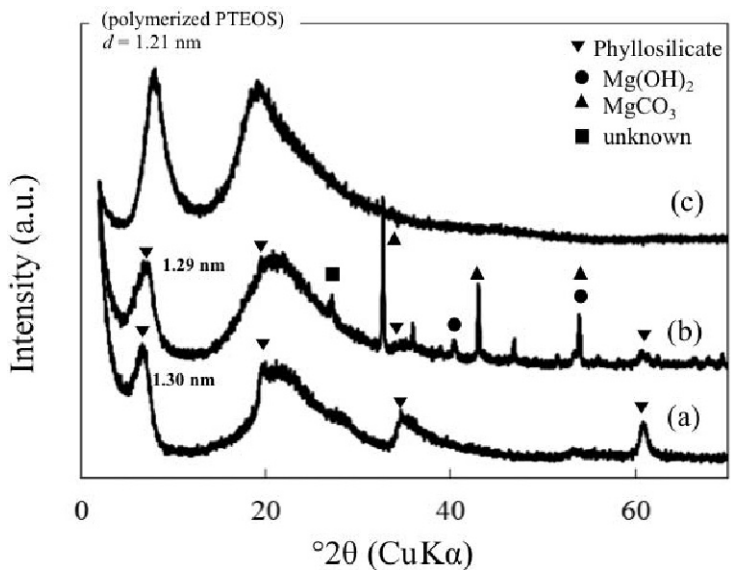

Figure 5. XRD patterns of: (a) Ph-0.04-4-H, (b) Ph-0.3-4-H, and (c) polymerized PTEOS.

https://doi.org/10.1346/CCMN.2018.064097 Published online by Cambridge University Press

(Burkett *et al*., 1997). The basal spacings of Ph-0.04-4-H and Ph-0.3-4-H were 1.3 nm (interlayer spacings of 0.3 nm). Considering the molecular thickness of phenyl groups (0.33 nm) (Webster *et al*., 1998), hydrolyzed PTEOS was, presumably, intercalated into the interlayer space with the molecular planes parallel to the silicate sheet. The addition of the larger amount of PTEOS (Ph-0.3-4-H) resulted in the coprecipitation of magnesium carbonate and hydroxide, as was observed in the XRD pattern (Figure 5b). Excess amounts of PTEOS may undergo copolymerization with dissolved silica oligomers, and thus probably only a small proportion of the dissolved silica participated in the formation of hectorite. The excess Mg ions were, therefore, thought to precipitate to form Mg carbonate and hydroxide in the presence of hydrolyzed urea.

The SEM images of the products shown in Figure 6 revealed that hectorite-like silicates grew selectively on silica spheres, because only spherical grains with a size of 2.7 μm covered with platy particles were observed. The platy particles in the PTEOS systems (Figure 6b,c) were larger than those in the MTEOS system (Figure 6a). The aspect ratio increased when the amount of PTEOS was increased to 0.3 mol/L mol SiO_2 (Ph-0.3-4-H: Figure 6c). The increase in crystallite size can be explained by a decline in oversaturation (nuclei) because silica oligomers were consumed by reacting with excess PTEOS.

The solid-state ^{29}Si MAS NMR spectra of the hydrothermal products are shown in Figure 7. Q*n* signals that were assigned to the silicate sheet of hectorite were observed at −110, −94, and −86 ppm for $Q_4(Si(OSi)_4)$, $Q_3(Si(OMg)(OSi)_3)$, and $Q_2(Si(OMg)(OSi)_2(OH))$, respectively (Fujii and Hayashi, 2005; Carrado *et al*., 2000, 2002). When the amount of MTEOS was increased to 0.3 mol/L mol SiO_2, the signals assigned to the $T_2'(RSi(OMg)(OSi)_2)$ and $T_1'(RSi(OMg)(OH)(OSi))$ environments at −67 and −60 ppm, respectively, became more intense (Figure7b) than those for the smaller amount of MTEOS (Figure 7a). Each T_n' signal was located in a higher-frequency region for polymerized MTEOS (Figure 7c). These results suggest an increase in the amount of grafted methyl groups.

For the PTEOS product (Ph-0.3-4-H), the signals (Figure 7e) observed at −79 and −67 ppm were assigned to the T_n' environments (Fujii and Hayashi,

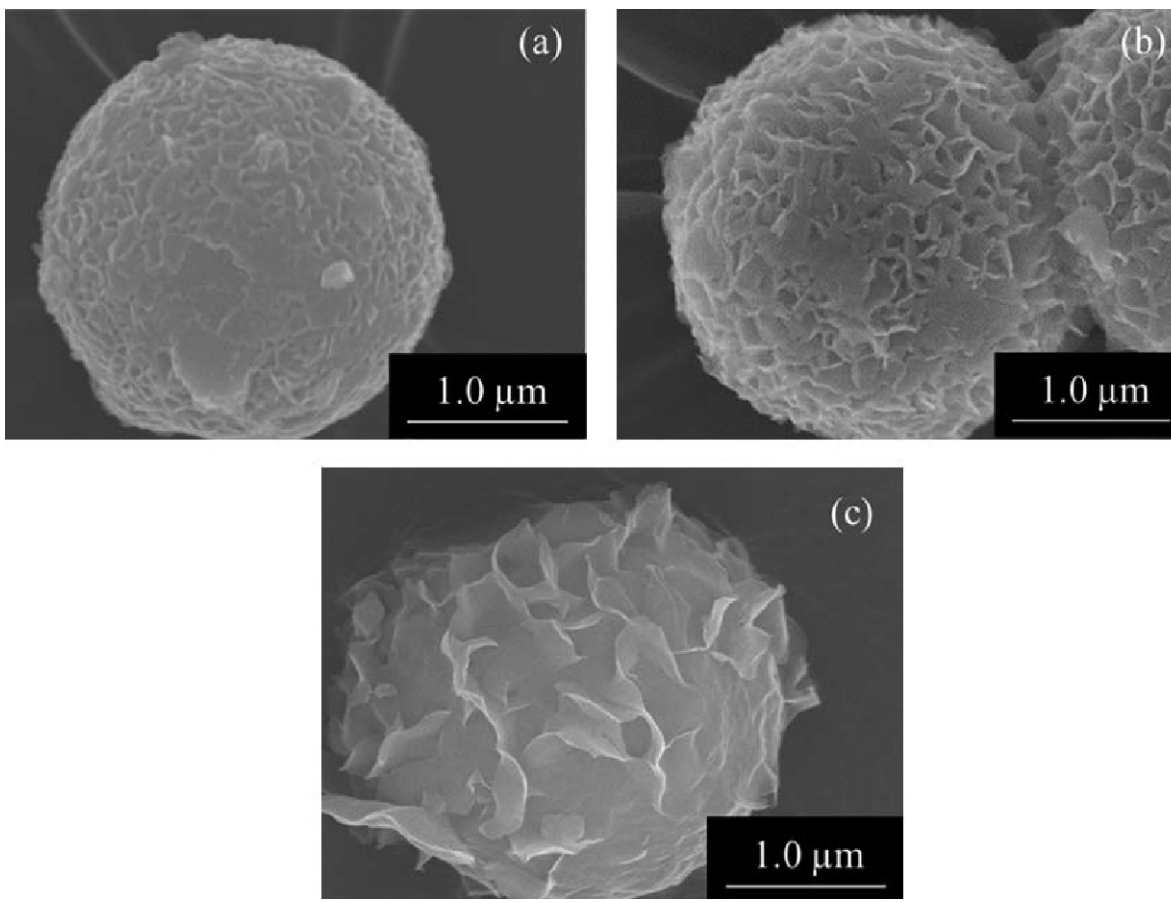

Figure 6. SEM images of: (a) Me-0.3-4-H, (b) Ph-0.04-4-H, and (c) Ph-0.3-4-H.

https://doi.org/10.1346/CCMN.2018.064097 Published online by Cambridge University Press

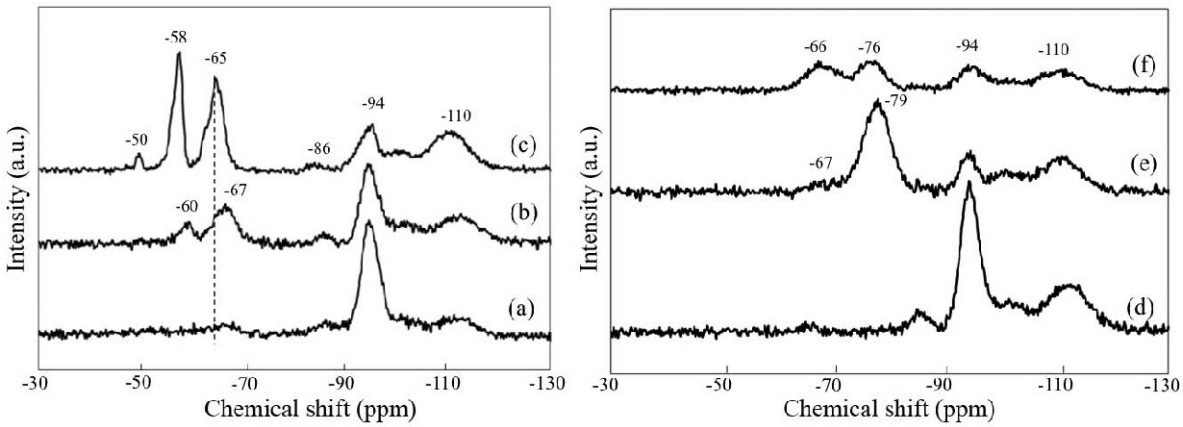

Figure 7. Solid-state ^{29}Si MAS NMR spectra of: (a) Me-0.04-4-H, (b) Me-0.3-4-H, (c) a mixture of polymerized MTEOS and Me-0-4-H, (d) Ph-0.04-4-H, (e) Ph-0.3-4-H, and (f) a mixture of polymerized PTEOS and Me-0-4-H.

2005) of T_2'(*R*Si(OMg)(OSi)$_2$) and T_1'(*R*Si(OMg)(OH)(OSi)) (Carrado *et al.*, 2001; Burkett *et al.*, 1997), respectively, because these were located in a lower-frequency region than those for the polymerized PTEOS shown in Figure 7f (−76 ppm for T_3(*R*Si(OSi)$_3$) and −66 ppm for T_2(*R*Si(OH)(OSi)$_2$) (Liu *et al.*, 2006). Phenylsilyl groups are thought to have been grafted onto phyllosilicate layers with a hectorite-like structure.

The results of the TG-DTA analyses of the grafted samples are summarized in Table 2. The mass loss in the temperature range of 200−800ºC was due to dehydration of structural hydroxyl groups and oxidative decomposition of organic groups. The methyl groups content in Me-0.04-4-H may be smaller, considering that the corresponding mass loss of 3% was similar to that for the unmodified sample (3% for Me-0-4-H). The increase in the amount of MTEOS (Me-0.3-4-H) led to an increase in the mass loss to 9%, which indicated an increase in the amount of grafted methylsilyl groups. In the PTEOS systems, the amount of grafted groups may also have increased with the increase in the amount of PTEOS, judging by the mass losses of 4% for Ph-0.04-4-H and 24% for Ph-0.3-4-H. The formation of porous structure in the interlayer space was confirmed by comparing the specific surface area listed in Table 2. The surface areas of the samples grafted with a small amount of organic groups (Me-0.04-4-H: 161 m^2/g, Ph-0.04-4-H: 116 m^2/g) were larger than that of the non-grafted sample (Me-0-4-H: 81 m^2/g). Dense packing of the organic moiety in the interlayer space is a possible reason for the decrease in the surface area.

On the bases of the XRD, SEM, TG-DTA, N_2 adsorption, and NMR analyses, the *in situ* crystallization of hectorite-like organosilicates derived by grafting organosilyl (methyl and phenyl) groups onto spherical silica particles was elucidated.

Adsorption of MB. The adsorption of a cationic dye (*i.e.* MB) onto the samples from an aqueous phase was studied. Because the adsorption of MB proceeds *via* cation-exchange reactions, the fraction of layered silicates in hybrid samples (*i.e.* the silicate/silica ratio) can be estimated from their cation-exchange capacity (Okada *et al.*, 2012b). According to the Giles (1974) classification, the adsorption isotherms were of L type. The adsorption isotherms were fitted to the Langmuir (1918) equation which is given as follows:

$$C_e/Q = (1/K_LQ_m) + (1/Q_m)C_e \quad (1)$$

where Q_m and K_L are constants related to the maximum amount adsorbed and maximum binding energy,

Table 2. Langmuir parameters for adsorption of MB and results of TG-DTA analyses of samples before adsorption of MB.

Sample	Langmuir parameter		r^2	Mass loss (%)		N_2 BET surface area (m^2/g)
	K_L (10^5 L mol^{-1})	Q_m (mmolg^{-}1)		25−100ºC	200−800ºC	
Me-0-4-H	0.75	0.47	0.99	5	3	81
Me-0.04-4-H	7.2	0.38	0.99	4	3	161
Me-0.3-4-H	8.6	0.26	0.99	5	9	132
Ph-0.04-4-H	1.7	0.44	0.99	5	4	116
Ph-0.3-4-H	0.11	0.17	0.97	1	24	14

https://doi.org/10.1346/CCMN.2018.064097 Published online by Cambridge University Press

respectively. Q and C_e denote the amount adsorbed and the equilibrium concentration, respectively. The Langmuir parameters derived from the adsorption isotherms are listed in Table 2. When the amount of MTEOS was increased, the maximum amount adsorbed, Q_m, decreased. The Langmuir adsorption constant, K_L, increased eventually and was particularly high for Me-0.3-4-H ($K_L = 8.6 \times 10^5$ L mol^{-1}). This indicates that the silicate sheet was modified with methylsilyl groups that enabled strong interactions with MB. In the PTEOS systems, the Q_m value also decreased with increase in the amount of PTEOS. The K_L value for Ph-0.3-4-H, on the other hand, was less than those for the unmodified sample (Me-0-4-H) and Ph-0.04-4-H.

An increase in the amount of grafted groups was associated with a decrease in the amount of water adsorbed, which was estimated from the mass losses observed in the temperature range 25–100ºC (5% for Ph-0.04-4-H and 1% for Ph-0.3-4-H) in the TG-DTA curves. Modification with phenylsilyl groups was known to impart hydrophobic properties. The increase in hydrophobicity (decrease in the amount of adsorbed water) due to the phenyl groups was a factor responsible for the decline in the adsorption of MB, which was presumably due to the dehydration of exchangeable cations in the interlayer. The determination of the fraction of layered silicate in the samples from the MB adsorption experiment was difficult, therefore.

CONCLUSIONS

Fine phyllosilicate crystals that were grafted with methylsilyl and phenylsilyl groups were grown on the surface of monodisperse spherical silica particles which were 2.6 μm in size. Hydrothermal reactions were performed at 100 and 150ºC in the presence of organosilanes (MTEOS and PTEOS), monodisperse silica spheres, $MgCl_2$, LiF, and urea for 2 or 4 days. The higher temperature was necessary for covalent attachment of silyl groups to silicate sheets and to preserve a uniform grain-size distribution. The longer reaction period led to greater crystallinity of the resulting organo-phyllosilicates. Excess organosilanes (0.5 mol/L mol SiO_2) participated in reactions with silica oligomers formed by the dissolution of the initial silica spheres, which resulted in the precipitation of magnesium carbonate and hydroxide and reduced the amount of phyllosilicates that were formed. The maximum amount of MB adsorbed decreased when the amount of organosilanes added was increased. The strength of adsorbate–adsorbent interactions (which was derived from the Langmuir K_L value) was different for the MTEOS and PTEOS systems, due, presumably, to the difference in the hydrophobicity of the organic moiety.

REFERENCES

Bailey, S.W., editor (1988) *Hydrous Phyllosilicates (exclusive of Micas)*. Reviews in Mineralogy, vol. **19**. Mineralogical Society of America, Washington D.C.

Burkett, S.L., Press, A., and Mann, S. (1997) Synthesis, characterization, and reactivity of layered inorganic–organic nanocomposites based on 2:1 trioctahedral phyllosilicates. *Chemistry of Materials*, **9**, 1071–1073.

Carrado, K.A., Xu, L., Gregory, D.M., Song, K., Seifert, S., and Botto, R.E. (2000) Crystallization of a layered silicate clay as monitored by small-angle X-ray scattering and NMR. *Chemistry of Materials*, **12**, 3052–3059.

Carrado, K.A., Xu, L., Csencsits, R., and Muntean, J.V. (2001) Use of organo- and alkoxysilanes in the synthesis of grafted and pristine clays. *Chemistry of Materials*, **13**, 3766–3773.

Carrado, K.A., Csencsits, R., Thiyagarajan, P., Seifert, S., Macha, S.M., and Harwood, J.S. (2002) Crystallization and textural porosity of synthetic clay minerals. *Journal of Materials Chemistry*, **12**, 3228–3237.

Chen, H., Zhang, F., Fu, S., and Duan X. (2006) Orientation-controlled monolayer assembly of zeolite crystals on glass and mica by covalent linkage of surface-bound epoxide and amine groups. *Advanced Materials*, **18**, 3089–3093.

Chhowalla, M., Shin, H.S., Eda, G., Li, L. J., Loh, K.P., and Zhang, H. (2013) The chemistry of two-dimensional layered transition metal dichalcogenide nanosheets. *Nature Chemistry*, **5**, 263–275.

Cool, P. and Vansant, E. F. (2004) Pillared clay and porous clay heterostructures. Pp. 261–311 in: *Handbook of Layered Materials* (S.M. Auerbach, K.A. Carrado, and P.K. Dutta, editors). CRC Press, Boca Raton, Florida, USA.

da Fonseca, M.G., Silva, C.R., and Airoldi, C. (1999) Aminated phyllosilicates synthesized via a sol-gel process. *Langmuir*, **15**, 5048–5055.

da Fonseca, M.G., Barone, J.S., and Airoldi, C. (2000a) Self-organized inorganic-organic hybrids induced by silylating agents with phyllosilicate-like structure and the influence of the adsorption of cations. *Clays and Clay Minerals*, **48**, 638–647.

da Fonseca, M.G., Silva, C.R., Barone, J.S., and Airoldi, C. (2000b) Layered hybrid nickel phyllosilicates and reactivity of the gallery space. *Journal of Materials Chemistry*, **10**, 789–795.

Fujii, K. and Hayashi, S. (2005) Hydrothermal syntheses and characterization of alkylammonium phyllosilicates containing $CSiO_3$ and SiO_4 units. *Applied Clay Science*, **29**, 235–248.

Fujii, K., Hayashi, S., and Kodama, H. (2003) Synthesis of an alkylammonium/ magnesium phyllosilicate hybrid nanocomposite consisting of a smectite-like layer and organosiloxane layers. *Chemistry of Materials*, **15**, 1189–1197.

Fukushima, Y. and Tani, M. (1995) An organic/inorganic hybrid layered polymer: methacrylate-magnesium (nickel) phyllosilicate. *Journal of Chemical Society; Chemical Communications*, **2**, 241–242.

Fukushima, Y. and Tani, M. (1996) Synthesis of 2:1 type 3-(methacryloxy) propyl magnesium (nickel) phyllosilicate. *Bulletin of the Chemical Society of Japan*, **69**, 3667–3671.

Giles, C.H., Smith, D., and Huitson, A. (1974) A general treatment and classification of the solute adsorption isotherm. *Journal of Colloid and Interface Science*, **47**, 755–765.

Jaber, M. and Miehe-Brendle, J. (2008) Synthesis, characterization and applications of 2:1 phyllosilicates and organophyllosilicates: Contribution of fluoride to study the octahedral sheet. *Microporous and Mesoporous Materials*, **107**, 121–127.

Jaber, M., Miehe-Brendle, J., Roux, M., Dentzer, J., Dred,

https://doi.org/10.1346/CCMN.2018.064097 Published online by Cambridge University Press

R.L., and Guth, J.L. (2002) A new Al, Mg-organoclay. *New Journal of Chemistry*, **26**, 1597–1600.

Jaber, M., Miehe-Brendle, J., Delmotte, L., and Dred, R.L. (2005) Formation of organoclays by a one-step synthesis. *Solid State Sciences*, 7, 610–615.

Katagiri, K., Goto, Y., Nozawa, M., and Koumoto, K. (2009) Preparation of layered double hydroxide coating films *via* the aqueous solution process using binary oxide gel films as precursor. *Journal of the Ceramic Society of Japan*, **117**, 356–358.

Kloprogge, J.T. (1998) Synthesis of smectites and porous pillared clay catalysts: A review. *Journal of Porous Materials*, **5**, 5–41.

Langmuir, I. (1918) The adsorption of gases on plane surface of glass, mica and platinum. *Journal of the American Chemical Society*, **40**, 1361–1403.

Liu, S., Ye, H., Zhou, Y., and Zhao, J. (2006) Hydrolytic co-condensation of phenyltriethoxysilane with γ-aminopropyltriethoxysilane in the presence of sodium dodecyl sulfate. *Polymer Journal*, **38**, 220–225.

Ogawa, M. and Kuroda, K. (1995) Photofunctions of intercalation compounds. *Chemical Reviews*, **9**, 399–438.

Ogawa, M., Okutomo, S., and Kuroda, K. (1998) Control of interlayer microstructures of a layered silicate by surface modification with organochlorosilanes. *Journal of the American of Chemical Society*, **120**, 7361–7362.

Okada, T. (2018) Direct crystallization of layered silicates on the surface of amorphous silica. *The Chemical Record*, DOI: 10.1002/tcr.201700071.

Okada, T. and Ogawa, M. (2017) Inorganic–organic interactions. Pp. 163–186 in: *Inorganic Nanosheets and Nanosheet-Based Materials* (T. Nakato, J. Kawamata, and S. Takagi, editors). Springer, Berlin.

Okada, T., Ide, Y., and Ogawa, M. (2012a) Organic-inorganic hybrids based on ultrathin oxide layers – designed nanostructures for molecular recognition. *Chemistry – An Asian Journal*, **7**, 1980–1992.

Okada, T., Yoshido, S., Miura, H., Yamakami, T., Sakai, T., and Mishima, S. (2012b) Swellable microsphere of a layered silicate produced by using monodispersed silica particles. *The Journal of Physical Chemistry C*, **116**, 21864–21869.

Okada, T., Seki, Y., and Ogawa, M. (2014) Designed nanostructures of clay for controlled adsorption of organic compounds. *Journal of Nanoscience and Nanotechnology*, **14**, 2121–2134.

Okada, T., Oguchi, J., Yamamoto, K., Shiono, T., Fujita, M., and Iiyama, T. (2015a) Organoclays in water cause expansion that facilitates caffeine adsorption. *Langmuir*, **31**, 180–187.

Okada, T., Suzuki, A., Yoshido, S., and Minamisawa, H.M. (2015b) Crystal architectures of a layered silicate on monodisperse spherical silica particles cause the topochemical expansion of the core-shell particles. *Microporous and Mesoporous Materials*, **215**, 168–174.

Okada, T., Sueyoshi, M., and Minamisawa, H. M. (2015c) In situ crystallization of Al-containing silicate nanosheets on monodisperse amorphous silica microspheres. *Langmuir*, **31**, 13842–13849.

Okada, T., Shimizu, K., and Yamakami, T. (2016a) An inorganic anionic polymer filter disc: Direct crystallization of a layered silicate nanosheet on a glass fiber filter. *RSC Advances*, **6**, 26130–26136.

Okada, T., Kobari, H., and Haeiwa, T. (2016b) Effects of fluoride and urea on the crystal growth of a hectorite-like layered silicate on a silica surface. *Applied Clay Science*, **132–133**, 320–325.

Okada, T., Kumasaki, A., Shimizu, K., Yamagishi, A., and Sato, H. (2016c) Application of hectorite-coated silica gel particles as a packing material for chromatographic resolution. *Journal of Chromatographic Science*, **54**, 1238–1243.

Okada, T., Yoshida, T., and Iiyama, T. (2017) Kinetics of interlayer expansion of a layered silicate driven by caffeine intercalation in the water phase using transmission X-ray diffraction. *The Journal of Physical Chemistry B*, **121**, 6919–6925.

Pérez-Carvajal, J., Aranda, P., Berenguer-Murcia, A., Cazorla-Amorós, D., Coronas, J., and Ruiz-Hitzky, E. (2013) Nanoarchitectures based on layered titanosilicates supported on glass fibers: Application to hydrogen storage. *Langmuir*, **29**, 7449–7455.

Pinnavaia, T.J., Tzou, M.S., Landau, S.D., and Raythatha, R. H. (1984) On the pillaring and delamination of smectite clay catalysts by polyoxo cations of aluminum. *Journal of Molecular Catalysis*, **27**, 195–212.

Rogez, G., Massobrio, C., Rabu, P., and Drillon, M. (2011) Layered hydroxide hybrid nanostructures: A route to multifunctionality. *Chemical Society Reviews*, **40**, 1031–1058.

Ruiz-Hitzky, E. and Rojo, J.M. (1980) Intracrystalline grafting on layer silicic acids. *Nature*, **287**, 28–30.

Ruiz-Hitzky, E., Rojo, J.M., and Lagaly, G. (1985) Mechanism of the grafting of organosilanes on mineral surfaces. *Colloid and Polymer Science*, **263**, 1025–1030.

Sugahara, Y., Okada, S., Sato, S., Kuroda, K., and Kato, C. (1994) ^{29}Si-NMR study of hydrolysis and initial polycondensation processes of organoalkoxysilanes. II. Methyltriethoxysilane. *Journal of Non-Crystalline Solids*, **167**, 21–28.

Thiesen, P., Beneke, K., and Lagaly, G. (2000) Alkylammonium derivatives of layered alkali silicates and micro- and mesoporous materials: I. Lithium sodium silicate (silinaite). *Journal of Materials Chemistry*, **10**, 1177–1184.

Thiesen, P., Beneke, K., and Lagaly, G. (2002) Silylation of a crystalline silicic acid: an MAS NMR and porosity study. *Journal of Materials Chemistry*, **12**, 3010–3015.

Webster, C.E., Drago, R.S., and Zerner, M.C. (1998) Molecular dimensions for adsorptives. *Journal of the American Chemical Society*, **120**, 5509–5516.

Whilton, N.T., Burkett, S.L., and Mann, S. (1998) Hybrid lamellar nanocomposites based on organically functionalized magnesium phyllosilicate clays with interlayer reactivity. *Journal of Materials Chemistry*, **8**, 1927–1932.

Yamaguchi, N., Nakamura, T., Tadanaga, K., Matsuda, A., Minami, T., and Tatsumisago, M. (2006) Direct formation of Zn-Al layered double hydroxide films with high transparency on glass substrate by the sol-gel process with hot water treatment. *Crystal Growth & Design*, **6**, 1726–1729.

Zhang, F., Zhao, L., Chen, H., Xu, S., Evans, D.G., and Duan, X. (2008) Corrosion resistance of superhydrophobic layered double hydroxide films on aluminum. *Angewandte Chemie International Edition*, **47**, 2466–2469.

Zhang, T., Zhou, Y., He, M., Zhu, Y., Bu, X., and Wang, Y. (2013) Biomimetic fabrication of hierarchically structured LDHs/ZnO composites for the separation of bovine serum albumin. *Chemical Engineering Journal*, **219**, 278–285.

Zhang, T., Zhou, Y., Bu, X., Xue, J., Hu, J., Wang, Y., and Zhang, M. (2014) Bio-inspired fabrication of hierarchically porous Mg-Al composites for enhanced BSA adsorption properties. *Microporous and Mesoporous Materials*, **188**, 37–45.

(*Received 21 October 2017; revised 23 April 2018; Ms. 1230; AE: M. Ogawa*)